

doi:10.15199/48.2023.03.50

# A Novel Simplified Model of Dual Motor Belt Drive for Modern Motorcycles and Low Speed Electric Vehicles

**Abstract.** Power transmission belt based dual motor drive becomes a future trend drive for modern motorcycles and low speed electric vehicles. However, there are only few research studies on this drive system due to their relatively new and complexity. This paper proposes a new simplified model for this power transmission belt drive of the dual motor electric vehicles. The proposed model was derived based on the mathematical and mechanical-electrical characteristics of the system. The proposed model was evaluated via the simulation and validated in comparison with the experimental vehicle and system prototype. The comparison results showed that the pro-posed model achieved good agreement for both steady state and dynamic responses of the actual drive system. This model could be applied for the chain and direct shaft drive system as well, which will be published in the next research papers.

**Streszczenie.** Napęd dwusilnikowy oparty na pasie transmisyjnym staje się przyszłościowym napędem dla nowoczesnych motocykli i pojazdów elektrycznych o małej prędkości. Istnieje jednak niewiele prac badawczych dotyczących tego układu napędowego ze względu na ich stosunkowo nowe i złożoność. W artykule zaproponowano nowy uproszczony model tego napędu pasowego przenoszenia mocy w dwusilnikowych pojazdach elektrycznych. Zaproponowany model został wyprowadzony na podstawie matematycznej i mechaniczno-elektrycznej charakterystyki układu. Zaproponowany model został oceniony za pomocą symulacji i poddany walidacji w porównaniu z eksperymentalnym pojazdem i prototypem systemu. Wyniki porównania wykazały, że proponowany model osiągnął dobrą zgodność zarówno dla stanu ustalonego, jak i odpowiedzi dynamicznych rzeczywistego układu napędowego. Model ten może być również zastosowany do układu napędu łańcuchowego i bezpośredniego wału, co zostanie opublikowane w kolejnych pracach badawczych. (Nowatorski uproszczony model podwójnego napędu pasowego silnika dla nowoczesnych motocykli i pojazdów elektrycznych o niskiej prędkości)

**Keywords:** power transmission belt drive, dual motor drive, simplified drive model, motorcycles, low speed electric vehicles

**Słowa kluczowe:** napęd pasowy, podwójny napęd silnikowy, uproszczony model napędu, motocykle, pojazdy elektryczne o małej prędkości

## Introduction

Motorcycles are the most used motor vehicles in the world compared to cars [1]. The power transmission chain drive (PTCD) is the most commonly used drive for motorcycles due to its relatively low cost and low power transmission loss (typically 3%) [2],[3]. However, the PTCD has some drawbacks in that it requires often maintenance (typically 300-500 km for chain adjustment and lubrication) [4]. Therefore, the less maintenance chain type such the O-Ring type was developed (typically 10,000 km per one maintenance); but it has relatively high cost [5]. More preferable solutions regarding less maintenance required (typically about 10,000 for regular checking and 70,000-80,000 km for adjustment or replacing), cost effective, less noises and cleaner systems would be the belt drive or the shaft drive [6]. However, the shaft drive requires higher power drive compared to the belt drive. This would lead the belt drive to be the most attractive drive system in many modern vehicles [7],[8].

However, heavy researches on the belt drive could be conducted in order to eliminate the power transmission losses to become more competitive compared to the chain drive, as well as, higher power density (power per weight) and fast dynamic responses. Therefore, many models of the belt drive system and components are highly needed for the preliminary studies and tests, in order to reduce the design and pretest costs [9].

One of the possible ways to increase power density and fast response for the belt drive, as well as, capability of more flexible power management and longer motors' lifetime would be by applying the other drives into it as suggested in [10],[11]. However, when considering in terms of capability of more flexible power management and longer motors' lifetime, the most suitable one would be by using the dual motor drive system [12]-[13]; like its successively used in many types of cars [14]-[17]. However, a clear analytical model for this drive system has not been available yet.

The key part of the dual motor drive is the coupling part, which is the core mechanical device of motorcycles or electric vehicles (EVs) that joints the motor shafts to the power transmission part and the vehicle's body [18]. This part is inherently complicated with many involved sub-components; especially, when using for several motor drives system such as dual motor drive systems [18],[19]. In [19], the schematic diagram for the powertrain of the dual motor with direct shaft drive is presented in Figure 1. The first differential (D1) is composed of side gears 1 and 2 (SG1 and SG2), a carrier and planetary gears, and a ring gear (RG) which outputs the torque. The torque is transmitted through a reduction gear and from there to a second differential (D2). This diagram was adapted and used to develop the simplified model proposed in this research.

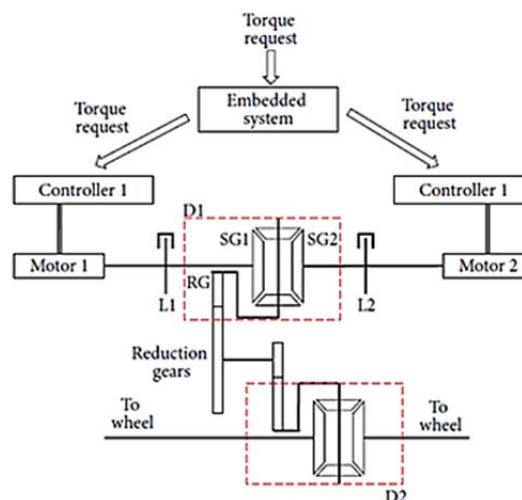
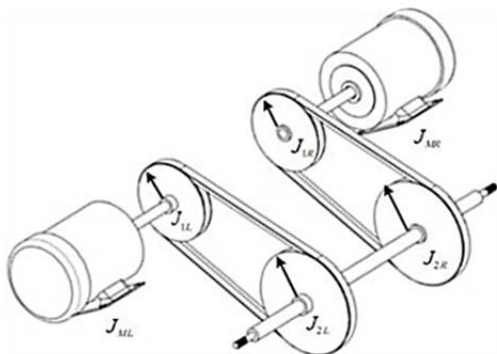


Fig.1. Schematic diagram of the propulsion module that shows the internal component of the transmission (differentials and gear reduction) and the motors, controllers, and embedded system [18],[19]

### Development of the Proposed Model

Figure 2(a)-(b) presents the simplified schematic model proposed in this research. The model was adapted from the diagram presented in Figure 1. The two motors (left motor and right motor with the subscript  $ML$  and  $MR$ ) are now represented by the moment of inertia. The motors are connected to the first pulleys (left pulley 1 and right pulley 1 as  $1L$  and  $1R$ ) and the first pulleys then transmit power from motor to the second pulleys (left pulley 2 and right pulley 2 as  $2L$  and  $2R$ ) via the left belt and the right belt, respectively. The power from the second pulleys is finally transmitted through the front wheels as shown in Figure 2(b). The photograph of the proposed simplified model prototype is illustrated in Figure 3.

a)



b)

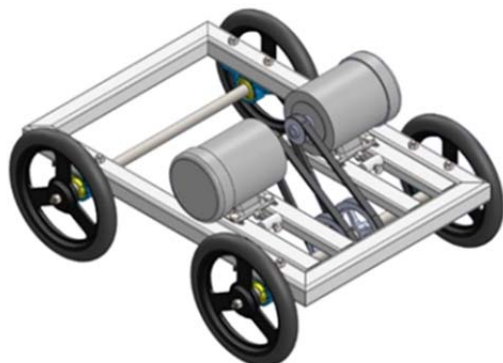


Fig.2. The simplified model of the dual motor belt drive system proposed in this research



Fig.3. Photograph of the proposed simplified dual motor belt drive model.

From Figure 3, two identical 764W induction motors were used and developed a 1.5kW power drive model. The model had a size with the width and length of 0.5 and 1.0 m, which is compact and ease to be used in the low cost laboratory study.

Based in the research analysis in [20], where the mechanical expression equations for the torque-speed relationship as shown in the equation (1):

$$(1) \quad T = \frac{T_L}{k_G} + J \frac{d}{dt} \omega + \beta \omega$$

where:  $J$  – equivalent system inertia,  $\beta$  – equivalent friction coefficient,  $\omega$  – angular speed of the motor shaft s.

According to the simplified dual motor belt drive system shown in Figure 2, the parameters of the left motor and the right motor components are substituted into the equation (1), which forms the equations (2) and (3):

$$(2) \quad T_{ML} = \frac{T_{L,ML}}{k_{G,ML}} + (J_{ML} + J_{1L} + J_{2L}) \frac{d}{dt} \omega_{ML} + \beta_{ML} \omega_{ML}$$

$$(3) \quad T_{MR} = \frac{T_{L,MR}}{k_{G,MR}} + (J_{MR} + J_{1R} + J_{2R}) \frac{d}{dt} \omega_{MR} + \beta_{MR} \omega_{MR}$$

where:  $T_{ML}$  – electrical torque of the left motor,  $T_{MR}$  – electrical torque of the right motor,  $T_{L,ML}$  – load torque of the left motor,  $T_{L,MR}$  – load torque of the right motor,  $J_{ML}$  – moment of inertia of the left motor,  $J_{MR}$  – moment of inertia of the right motor,  $J_{1L}$  – moment of inertia of the first pulley left side,  $J_{1R}$  – moment of inertia of the first pulley right side,  $J_{2L}$  – moment of inertia of the second pulley left side,  $J_{2R}$  – moment of inertia of the second pulley right side,  $k_{G,ML}$  – conversion ratios of the belt and pulley at left motor,  $k_{G,MR}$  – conversion ratios of the belt and pulley at right motor,  $\beta_{ML}$  – friction coefficient of the left motor,  $\beta_{MR}$  – friction coefficient of the right motor,  $\omega_{ML}$  – angular speed of the left motor,  $\omega_{MR}$  – angular speed of the right motor

Define  $T_M$  as the apparent torque of the drive system; where  $T_M = T_{ML} + T_{MR}$  This yields the equation (4):

$$(4) \quad T_M = \left( \frac{T_{L,ML}}{k_{G,ML}} + (J_{ML} + J_{1L} + J_{2L}) \frac{d}{dt} \omega_{ML} + \beta_{ML} \omega_{ML} \right) + \left( \frac{T_{L,MR}}{k_{G,MR}} + (J_{MR} + J_{1R} + J_{2R}) \frac{d}{dt} \omega_{MR} + \beta_{MR} \omega_{MR} \right)$$

As the conversion ratio between the belt and pulley is identical (unity); therefore  $k_G=1$  and the equation (4) can be simplified as (5)

$$(5) \quad T_M = \left( T_{L,ML} + (J_{ML} + J_{1L} + J_{2L}) \frac{d}{dt} \omega_{ML} + \beta_{ML} \omega_{ML} \right) + \left( T_{L,MR} + (J_{MR} + J_{1R} + J_{2R}) \frac{d}{dt} \omega_{MR} + \beta_{MR} \omega_{MR} \right)$$

As the wheels of the model do not contact to the floor for this research observation; therefore, the friction force can be ignored, by mean of  $\beta \approx 0$ , and the terms in the equation (5) can be further simplified as the equation (6).

$$(6) \quad T_M = \left( T_{L,ML} + (J_{ML} + J_{1L} + J_{2L}) \frac{d}{dt} \omega_{ML} \right) + \left( T_{L,MR} + (J_{MR} + J_{1R} + J_{2R}) \frac{d}{dt} \omega_{MR} \right)$$

As the two motors share the same load torque ( $T_{L,ML} = T_{L,MR}$ ) while they move with the same speed as the vehicle ( $\omega_{ML} = \omega_{MR}$ ). Thus, the equation (7) can be derived:

$$(7) \quad T_M = T_L + (J_{ML} + J_{1L} + J_{2L} + J_{MR} + J_{1R} + J_{2R}) \frac{d}{dt} \omega$$

where:  $T_L$  – total load torque of both motors,  $\omega$  – angular speed of both motors

If both motors are identical in shape, weight and size, as well as, the first pulleys (1L and 1R) are identical while the second pulleys (2L and 2R) are also identical, the terms JML will be assumed to be equal to JMR. Similarly, J1L will equal to J1R and J2L will equal to J2R, which yields the equation (8);

$$(8) \quad T_M = T_L + 2(J_M + J_1 + J_2) \frac{d}{dt} \omega$$

where  $J_M = J_{MR} = J_{ML}$ ,  $J_1 = J_{1L} = J_{1R}$ , and  $J_2 = J_{2L} = J_{2R}$

From the equation (8), the angular velocity differential equation can be derived as the equation (9):

$$(9) \quad \frac{d}{dt} \omega = \frac{T_M - T_L}{2(J_M + J_1 + J_2)}$$

The mathematical model of the dual motor belt drive has been now derived. Only the values of the physical parameters  $J_M$ ,  $J_1$  and  $J_2$  that could be determined as follows:

$J_M$  could be directly read from the motors' specific datasheet, as equation (10):

$$(10) \quad J_M = \text{data \{specification datasheet\}}$$

The pulleys has the flat cylindrical shape and thus  $J_1$  and  $J_2$  could be derived as the equations (11) and (12):

$$(11) \quad J_1 = \frac{1}{2} m_1 r_1^2$$

$$(12) \quad J_2 = \frac{1}{2} m_2 r_2^2$$

Where:  $m_1$ ,  $m_2$  – weight of pulley 1 and pulley 2,  $r_1$ ,  $r_2$  – radius of pulley 1 and pulley 2.

In this research, dual three phase ac induction motors were used. When implemented in the simulation program base on the math mathematical equations of a three-phase induction motor can be described in the stator fixed reference frame (stationary frame) by voltage equations can be written as follows [21]- [24] as expressed by equations (13)-(19):

$$(13) \quad [\mathbf{V}_s^{\alpha\beta 0}] = R_s [\mathbf{i}_s^{\alpha\beta 0}] + \frac{d}{dt} [\boldsymbol{\psi}_s^{\alpha\beta 0}]$$

$$(14) \quad [\mathbf{V}_{r'}^{\alpha\beta 0}] = R_r' [\mathbf{i}_{r'}^{\alpha\beta 0}] + \omega_r \begin{bmatrix} 0 & 1 & 0 \\ -1 & 0 & 0 \\ 0 & 0 & 0 \end{bmatrix} [\boldsymbol{\psi}_{r'}^{\alpha\beta 0}] + \frac{d}{dt} [\boldsymbol{\psi}_{r'}^{\alpha\beta 0}]$$

$$(15) \quad \begin{bmatrix} \boldsymbol{\psi}_s^{\alpha\beta 0} \\ \boldsymbol{\psi}_{\beta s} \\ \boldsymbol{\psi}_{0s} \end{bmatrix} = \begin{bmatrix} L_s \mathbf{i}_{\alpha s} + L_m \mathbf{i}'_{\alpha r} \\ L_s \mathbf{i}_{\beta s} + L_m \mathbf{i}'_{\beta r} \\ L_{ls} \mathbf{i}_{0s} \end{bmatrix}$$

$$(16) \quad \begin{bmatrix} \boldsymbol{\psi}_{r'}^{\alpha\beta 0} \\ \boldsymbol{\psi}'_{\beta r} \\ \boldsymbol{\psi}'_{0r} \end{bmatrix} = \begin{bmatrix} L_r' \mathbf{i}'_{\alpha r} + L_m \mathbf{i}_{\alpha s} \\ L_r' \mathbf{i}'_{\beta r} + L_m \mathbf{i}_{\beta s} \\ L_{lr}' \mathbf{i}'_{0r} \end{bmatrix}$$

$$(17) \quad L_s = L_{ls} + L_m$$

$$(18) \quad L_r' = L_{lr}' + L_m$$

$$(19) \quad T_e = \frac{3}{2} P (\boldsymbol{\psi}_{\alpha s} \mathbf{i}_{\beta s} - \boldsymbol{\psi}_{\beta s} \mathbf{i}_{\alpha s})$$

where:  $R_s$  – stator resistance,  $R_r'$  – rotor resistance,  $L_s$  – stator leakage inductance,  $L_r'$  – rotor leakage inductance,  $L_m$  – mutual inductance,  $L_{ls}$  – stator winding leakage inductance,  $L_{lr}'$  – rotor winding leakage inductance,  $\mathbf{V}_s^{\alpha\beta 0}$  – stator voltage on  $\alpha\beta$ -axis,  $\mathbf{V}_{r'}^{\alpha\beta 0}$  – rotor voltage on  $\alpha\beta$ -axis,  $\mathbf{i}_s^{\alpha\beta 0}$  –  $\alpha\beta$ -axis stator current,  $\mathbf{i}_{r'}^{\alpha\beta 0}$  –  $\beta$ -axis rotor current,  $i_{\alpha s}$  –  $\alpha$ -axis stator current,  $i'_{\alpha r}$  –  $\alpha$ -axis rotor current,  $i_{\beta s}$  –  $\beta$ -axis stator current,  $i'_{\beta r}$  –  $\beta$ -axis rotor current,  $i_{0s}$  – zero-sequence stator current,  $i'_{0r}$  – zero-sequence rotor current,  $\boldsymbol{\psi}_s^{\alpha\beta 0}$  –  $\alpha\beta$ -axis stator flux linkages,  $\boldsymbol{\psi}_{r'}^{\alpha\beta 0}$  –  $\alpha\beta$ -axis rotor flux linkages,  $\boldsymbol{\psi}_{\alpha s}$  –  $\alpha$ -axis stator flux linkages,  $\boldsymbol{\psi}'_{\alpha r}$  –  $\alpha$ -axis rotor flux linkages,  $\boldsymbol{\psi}_{\beta s}$  –  $\beta$ -axis stator flux linkages,  $\boldsymbol{\psi}'_{\beta r}$  –  $\beta$ -axis rotor flux linkages,  $\boldsymbol{\psi}_{0s}$  – zero-sequence stator flux linkages,  $\boldsymbol{\psi}'_{0r}$  – zero-sequence rotor flux linkages,  $\omega_r$  – electrical speed (rotor speed),  $T_e$  – electromagnetic torque,  $P$  – pole pairs.

## Results and Discussion

### A. Simulation Model

Figure 4 shows the overall simulation circuit diagram of the simulation system under this research. The circuit diagram composed of 2 three-phase ac power supply sources, two motor modules and the proposed simplified dual motor belt drive model. Figure 5 shows the zoomed-in circuit diagram of the simplified model, which was constructed by utilizing the derived equation (9) from the previous section. Figure 6 shows the circuit diagram of the motor module, which was used for both the left and right motors. The motor module utilized the equations (13)-(19) for

developing the simple block diagrams while the parameters used for the simulation tests are presented in Table 1. These parameters were extracted from the actual motors used in the experimental prototypes and the drive system. Both simulation model and the experimental test-rig were tested on the open loop control mode so that the real reaction and behaviour of the drive system could be directly compared.

The moment of inertia of the motors ( $J_M$ ) could be found from the manufacturing datasheet, which was  $0.0032 \text{ kg}\cdot\text{m}^2$  for this case study. The parameters in Table 1 were used to determine the moment of inertia of the first pulleys and the second pulleys by using the equation (11) and (12). From Table 1, the radius of the first and second pulley were 3.81

and 7.62 cm. while their weight were 0.3 kg. and 0.5 kg., respectively, when using the equations (11) and (12), the resultant could be obtained as follows:

$$J_M=0.0032 \text{ kg.m}^2; J_1=0.018 \text{ kg.m}^2 \text{ and } J_I=0.015 \text{ kg.m}^2$$

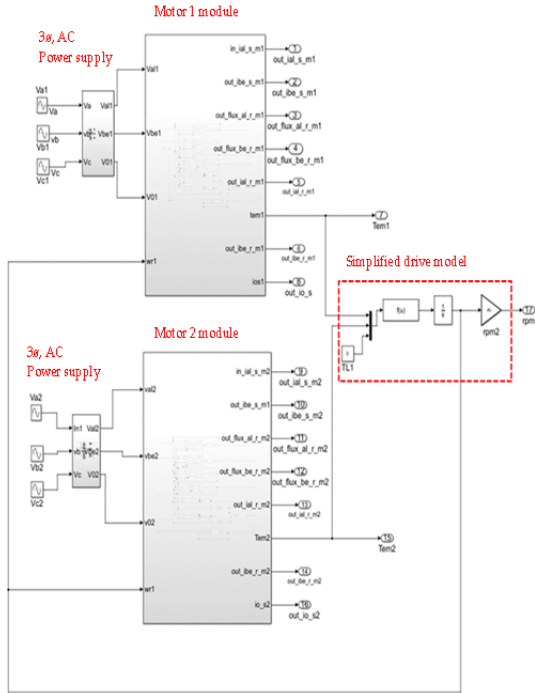


Fig.4. Simulation circuit diagram of the dual motor belt drive system using MATLAB-Simulink.

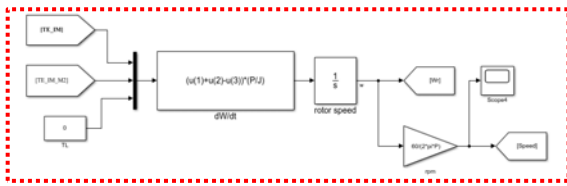


Fig.5. Simulation circuit diagram of the proposed Simplified dual motor belt drive using MATLAB-Simulink

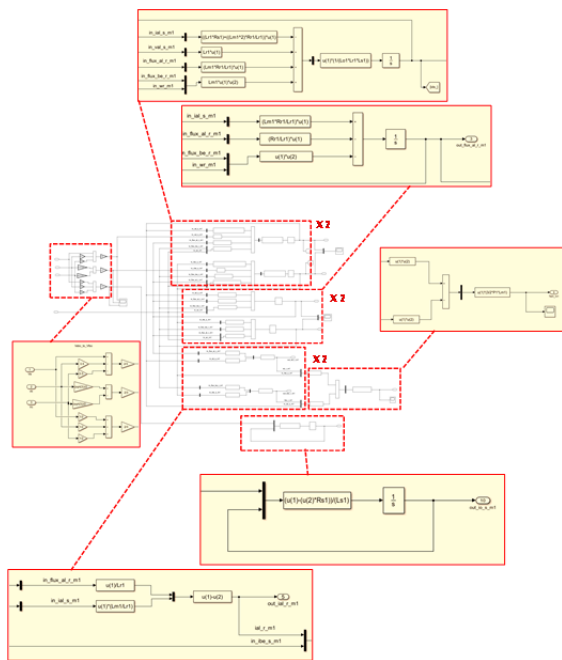


Fig.6. Simulation circuit components of the Motor 1 and Motor 2 modules using MATLAB-Simulink

Table 1. Test parameters and their values

Symbol	values
$R_s$	8.4 $\Omega$
$R_r$	8.59 $\Omega$
$L_{ls}$	0.0292 H
$L_{lr}$	0.0438 H
$L_m$	0.6958 H
$P$	2
$r_{1L}, r_{1R}$	3.81 cm.
$R_{2L}, r_{2R}$	7.6 cm.
$m_1$	0.3 kg.
$m_2$	0.5 kg.

### B. Experimental Test-Rig

Figure 7 presents the experimental test-rig used for the validation of the proposed simplified dual motor belt drive system.



Fig.7. Experimental Test-rig for the dual motor belt drive in the laboratory study.

### C. Test Results

Figure 8 shows the speed-time characteristics curves obtained from the tests of the simulation model (MATLAB-Simulink) and of the experimental test-rig under the open loop control. It can be seen that the proposed simplified model provides similar dynamic result to the experimental test-rig. However, there is some error during the start of the simulation which is the consequential result of the simplification; where the internal friction torque ( $\beta \approx 0$ ) was assumed to be ignored. The more precise model could be therefore taken into consideration for dynamic response study. However, for the steady state study, the simplified model could provide similar result to the experimental test-rig, as shown in Figures 9 and 10; where the stator current and the motor current obtained from the simulation model and experimental test-rig are presented.

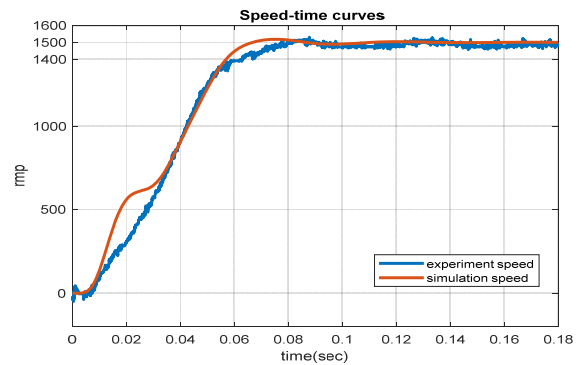


Fig.8. Comparison of speed-time curves between the simulation and experimental test-rig of the proposed dual motor belt drive.

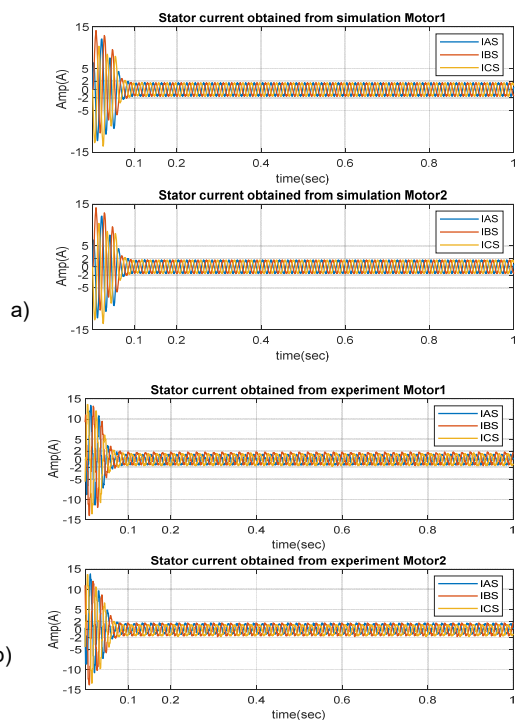


Fig.9. Stator current for both motors obtained from (a) MATLAB-Simulink simulation and (b) experiment test-rig.

## Conclusions

The Simplified Model of Dual Motor Belt Drive prototype for the 1.5 kW dual motor drive system was constructed and then used to verify the feasibility of the model. The test results for the motor current and motor speed values were compared between the simulation results and the experimental test results confirmed that the proposed model provided similar performance and characteristics to the one used in the experimental.

*Acknowledgments* This research was financially supported by Maharakham University (grant year 2021). The authors would like to thank for the supporting equipment and tools from Electric Automotive and Energy Technology Research Unit, Faculty of Engineering, Maharakham University, Thailand.

**Authors:** Ms. Wilaiporn Ngermbath. [wilaiporn.ng.ng@rmuti.ac.th](mailto:wilaiporn.ng.ng@rmuti.ac.th) Maharakham University., Assoc. Prof. Dr. Chonlatee Photong. [chonlatee.p@msu.ac.th](mailto:chonlatee.p@msu.ac.th) Maharakham University.

## REFERENCES

- [1] H. Rangkuti, J. Manalu and F. Fahmi, "Design of Efficient Electric Motorcycle Using Brushless DC Motor," 2020 4rd International Conference on Electrical, Telecommunication and Computer Engineering (ELTICOM), 2020, pp. 201-204, doi: 10.1109/ELTICOM50775.2020.9230505.
- [2] S. P. Zhang and T. O. Tak, "Efficiency estimation of roller chain power transmission system," Applied Sciences (Switzerland), vol. 10, no. 21. pp. 1–13, 2020, doi: 10.3390/app10217729
- [3] S. P. Zhang and T. O. Tak, "Efficiency evaluation of electric bicycle power transmission systems," Sustainability (Switzerland), vol. 13, no. 19. 2021, doi: 10.3390/su131910988.
- [4] De Rossi, L., Schramm, A., & De Felice, A. (2022). Multibody Efficiency Analysis of Chain Drives in Racing Motorcycles. *Journal of Applied and Computational Mechanics*, 8(3), 1091–1102. <https://doi.org/10.22055/jacm.2022.39795.3467>
- [5] Maleque MA, Rahman MM, Hossain MS. Reverse Engineering of Motorcycle Chain. *AMR* 2011;264–265:1678–83. <https://doi.org/10.4028/www.scientific.net/amr.264-265.1678>.
- [6] H. Zhu, W. D. Zhu, and W. Fan, "Dynamic modeling, simulation and experiment of power transmission belt drives: A

systematic review," *Journal of Sound and Vibration*, vol. 491. 2021, doi: 10.1016/j.jsv.2020.115759.

- [7] M. di Napoli, M. Strähle, S. Ruzimov, L. D. S. Cabrera, N. Amati, and A. Tonoli, "Intelligent Belt Drive Systems in Hybrid Powertrains: a Multipurpose Test Rig," *IFAC-PapersOnLine*, vol. 49, no. 21. pp. 47–53, 2016, doi: 10.1016/j.ifacol.2016.10.509.
- [8] J. -C. Guan, B. -C. Chen, Y. -D. Huang and Y. -J. Chiu, "Adaptive power management strategy for Hybrid Electric Vehicle with Belt-driven Starter Generator," 2015 IEEE 12th International Conference on Networking, Sensing and Con-trol, 2015, pp. 503-508, doi: 10.1109/ICNSC.2015.7116088
- [9] Y. Wu, M. J. Leamy, and M. Varenberg, "Belt-Drive Mechanics: Friction in the Absence of Sliding," *Journal of Applied Mechanics*, vol. 86, no. 10, Jun. 2019.
- [10] B. Tabbache, A. Kheloui, and M. E. H. Benbouzid, "An adaptive electric differential for electric vehicles motion stabilization," *IEEE Transactions on Vehicular Technology*, vol. 60, no. 1. pp. 104–110, 2011, doi: 10.1109/TVT.2010.2090949.
- [11] J. Y. A. R. K. B. Utkal Ranjan Muduli, Abdul R. Beig, Khaled Al Jaafari, "Interrupt Free Operation of Dual Motor Four Wheel Drive Electric Vehicle Under Inverter Failure.pdf." *IEEE TRANSACTIONS ON TRANSPORTATION ELECTRICIFICATION*, 2021
- [12] Y. L. Xiaosong Hu, Yapeng Li, Chen Lv, "Optimal Energy Management and Sizing of a Dual Motor Driven Electric Powertrain.pdf." *IEEE TRANSACTIONS ON POWER ELECTRONICS*, 2019.
- [13] S. Zhang, C. Zhang, G. Han, and Q. Wang, "Optimal Control Strategy Design Based on Dynamic Programming for a Dual-Motor Coupling-Propulsion System," *Scientific World Journal*, vol. 2014. 2014, doi: 10.1155/2014/958239
- [14] J. Y. A. R. K. B. Utkal Ranjan Muduli, Abdul R. Beig, Khaled Al Jaafari, "Interrupt Free Operation of Dual Motor Four Wheel Drive Electric Vehicle Under Inverter Failure.pdf." *IEEE TRANSACTIONS ON TRANSPORTATION ELECTRICIFICATION*, 2021.
- [15] Y. L. Xiaosong Hu, Yapeng Li, Chen Lv, "Optimal Energy Management and Sizing of a Dual Motor Driven Electric Powertrain.pdf." *IEEE TRANSACTIONS ON POWER ELECTRONICS*, 2019.
- [16] S. Zhang, C. Zhang, G. Han, and Q. Wang, "Optimal Control Strategy Design Based on Dynamic Programming for a Dual-Motor Coupling-Propulsion System," *Scientific World Journal*, vol. 2014. 2014, doi: 10.1155/2014/958239.
- [17] P. Panmuang, T. Thongsan, N. Suwapaet, J. Laohavanich, and C. Photong, "A novel dual motor drive system for three wheel electric vehicles," *AIP Conference Proceedings*, vol. 1941. 2018, doi: 10.1063/1.5028077.
- [18] J. Hu, L. Zheng, M. Jia, Y. Zhang, and T. Pang, "Optimization and Model Validation of Operation Control Strategies for a Novel Dual-Motor Coupling-Propulsion Pure Electric Vehicle," *Energies*, vol. 11, no. 4, p. 754, Mar. 2018.
- [19] P. D. Urbina Coronado and H. Ahuett-Garza, "Control Strategy for Power Distribution in Dual Motor Propulsion System for Electric Vehicles," *Mathematical Problems in Engineering*, vol. 2015. 2015, doi: 10.1155/2015/814307.
- [20] Jafarboland and J. Faiz, "Modelling and designing controller of two different mechanical coupled motors for enhancement of underwater vehicles performance," *IET Electric Power Applications*, vol. 4, no. 7. pp. 525–538, 2010, doi: 10.1049/iet-epa.2010.0005.
- [21] Chee-Mun Ong, *Dynamic Simulations of Electric Machinery: Using MATLAB/SIMULINK*. PRENTICE HALL PTR, 1997.
- [22] K. T. Chau, "Electric Vehicle Machines and Drives," *Electric Vehicle Machines and Drives*. 2015, doi: 10.1002/9781118752555.
- [23] P. SIRIKAN, "Implementation of Indirect Rotor Field Oriented Control for Three- Phase Induction Motor Drive based on TMS320F28335 DSP," *PRZEGLĄD ELEKTROTECHNICZNY*, vol. 1, no. 9, pp. 155–160, Sep. 2020.
- [24] A. S. P. Sawatnatee, S. Udomsuk, K-N. Areerak, K-L. Areerak, "the optimal indirect vector controller design via an adaptive tabu search algorithm." *World Academy of Science, Engineering and Technology International Journal of Computer and Systems Engineering*.